

# SWITCHING SURGES BY VACUUM CIRCUIT BREAKER, AND PROTECTION GUIDE

Katsushi Nagami  
Shoji Honma  
Susumu Tabata  
Hirotoshi Sasaki  
Isamu Okada  
Yasumasa Umesato  
Masayoshi Mitani

## I. FOREWORD

In retrospect, it can be seen that protection method against switching surges due to interruptions by vacuum circuit breakers (called VCB hereinafter) advanced technologically with advancement of the analysis of the surge generating processes.

When the VCB first appeared on the market, the abnormal voltage was recognized as a problem of high voltage peak value caused by current chopping. Then, from analysis of the voltage escalation phenomena caused by multiple reignition, the peak voltage and rising rate of high frequency voltage was seen to be dangerous and motor protection was especially emphasized in this respect. Therefore, as the protection method a lightning arrester for peak cut of chopping surge counter was adopted at first and next, a C-R surge absorber was adopted to reduce the rising rate of surge voltage, and a series reactor was adopted at some parts for the same purpose. Theoretically, the C-R system is desirable, but dimensions and cost are a problem compared to the peak cut system.

This investigation and measurement clarified the potential distribution in the motor winding for proceeding surge and clearly showed that peak cut surge absorber also can provide adequate motor protection if the residual voltage of this absorber is suitably selected.

The article reports on the results of the investigation and measurements on this theme and details the protection method using a newly commercialized peak cut type surge absorber based on these results.

## II. SWITCHING SURGE GENERATING PROCESS AND ANALYSIS

There are three kinds of switching surges caused by VCB, current chopping surge at low current interruption, surge due to multiple reignition at higher current interruption, and surge by pre-striking arc at closing operation. However, since the dielectric strength of a vacuum is very high compared to the circuit voltage, and the pre-strike time is so short that surge by pre-striking poses no problem.

The following describes the surges at interruption.

### 1. Current chopping surge

When a low current is interrupted, the arc before the current zero is unstable and the current is forcedly chopped. At this time, the energy remaining in the load inductance generates a surge. This surge is divided into the following two kinds by the relationship between the surge and the dielectric strength of the VCB.

#### 1) Chopping surge not accompanied with reignition

This is observed when the breaking current is larger than the VCB inherent chopping current. In this case, current chopping occurs after that arc has continued for a certain time and the distance between the VCB poles has reached a certain value, and the surge voltage given by the following equation occurs, not accompanied with reignition.

$$e_s = e^{-\frac{t}{\tau}} \cdot \sqrt{E^2 + (Z \cdot I_C)^2} \cdot \sin \omega t \quad \dots \dots \dots (1)$$

Where,  $\tau = 2RC$ ,  $Z = \sqrt{L/C}$ ,  $\omega \simeq 1/\sqrt{LC}$  (when  $R \gg Z/2$ )

$I_C$  = Chopping current,  $E$ : Phase voltage peak value

$L, C, R$  = Parallel load inductance, capacitance and resistance

From Eq. (1),  $e_s$  becomes lower as the load surge impedance  $Z$  becomes lower and the attenuation becomes faster as the parallel resistance  $R$  becomes smaller. As a VCB characteristics, the lower the chopping current  $I_C$  determined by the electrode material, the better. This chopping current also depends on the circuit conditions and generally tends to become smaller as the breaking current becomes larger or the surge impedance becomes larger.

#### 2) Chopping surge suppressed by reignition

This is seen when the breaking current is smaller than the VCB inherent chopping current, or the instantaneous current value at opening is small even when the breaking current is about the same as the chopping current. In this case, current chopping occurs immediately after opening and the VCB electrode distance is still short. Therefore, the chopping surge causes reignition, the choppings and reignitions are repeated several times, and at last the surge reaches the value of Eq. (1).

Fig. 1 shows a typical example. Since such a surge is suppressed by the VCB itself and the energy of the inductance is gradually dissipated in breaking arc,  $I_C$  at Eq. (1)

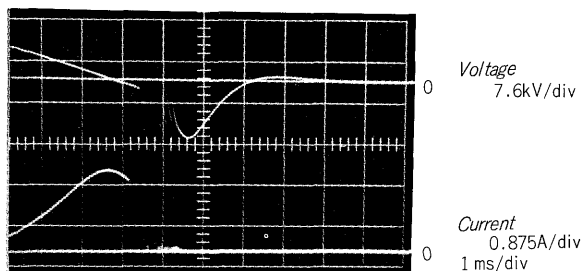


Fig. 1 Chopping surge suppressed by reignitions

becomes equivalently smaller.

Therefore, they VCB characteristic that determines this peak value of surge is the dielectric recovery characteristic more than the chopping current.

## 2. Multiple reignition surge

Even when the breaking current is comparatively large, from several tens to several hundred amperes, and the current chopping surge is not problem, a large surge may be generated when interrupting an inductive current, such as the starting current of a motor, for example. This is caused by the so-called multiple reignition surge. The surge is described by dividing it into the following two types.

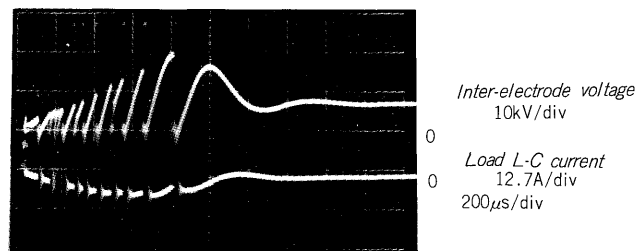
### 1) Multiple reignition surge at first interrupted pole

This surge is generated by repeated reignition at first pole interruption of three poles, when the contacts are opened immediately before the current zero point and the inter-electrode dielectric strength after the arc quenching is not enough. The difference between this type and type 2) of item 1 of para. II is that the inductance energy tends to become large at the initial stage and, therefore, an extremely large surge is generated.

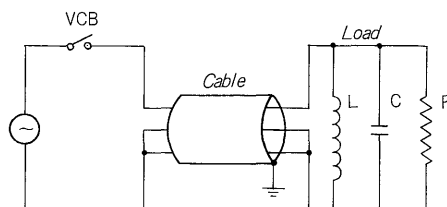
Fig. 2 shows a typical waveform at a single phase circuit. The surge increases along the dielectric recovery curve of the VCB. In this example, the final peak voltage is lower than the VCB dielectric strength and the escalation of the surge terminates. But, in the other example, the surge may terminate with the continuous arc of the half cycle supply current. The load L-C current  $i_L$  at the initial stage during the surge increases at the same  $di/dt$  as the breaking current. At reignition, the high frequency current (0.1 ~ several MHz) from the cable superimposed on  $i_L$  flows through VCB and interruption occurs at the point at which this current reaches zero. At this time  $i_L$  becomes virtually chopped and a large chopping surge is generated. However,  $i_L$  tends to decrease from a certain point and the surge terminates. The surge voltage applied to the load includes two components, a virtual chopping surge (several kHz) and a reignition surge (0.1 ~ several MHz). The latter component is a special problem at interturn insulation in windings.

### 2) Surge by 3-phase simultaneous interruption

Even when a multiple reignition surge is generated at first interrupted pole, there is usually no problem in the



(a) Waveform



(b) Circuit

Fig. 2 Multiple reignition surge

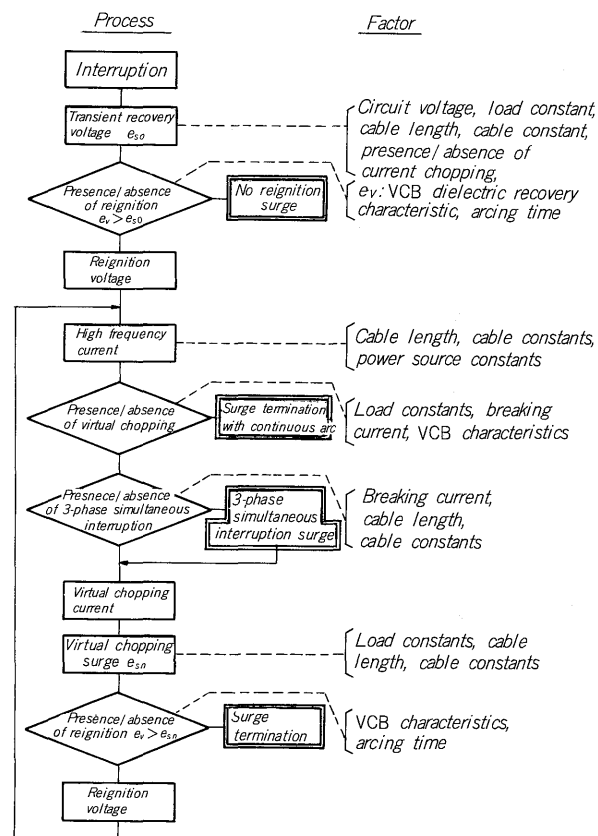


Fig. 3 Process and factors of multiple reignition surge

other two poles because of longer arcing time. However, if the reignition voltage at first pole increases and the high frequency current flowing into the other poles becomes large accompanying this, the supply current at the two poles is virtually chopped and a multiple reignition surge arises. This is called 3-phase simultaneous interruption surge, and since the reignition voltage becomes the value of

two poles of VCB connected in series, a surge larger than that of 1) is generated.

Fig. 3 summarizes the surge generation process and causes for cases 1) and 2) above. The main causes are described in the actual load experiment section.

### III. SURGE MEASUREMENT AND ANALYSIS AT THE INTERRUPTION TESTS OF ACTUAL LOAD CURRENT

The interruption tests were performed by using actual induction motors and molded power transformers as loads of VCB. The results of surge measurements and some analyses of surge problems are reported in the following.

#### 1. Motor load

##### 1) Surge measurement results

Fig. 4 shows the interruption test circuit of starting cur-

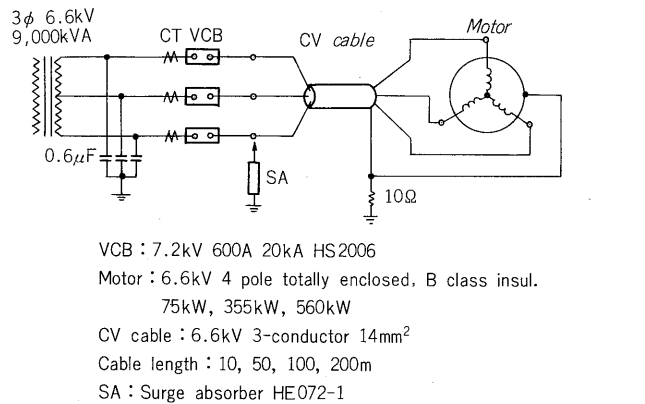


Fig. 4. Test circuit of induction motor switching

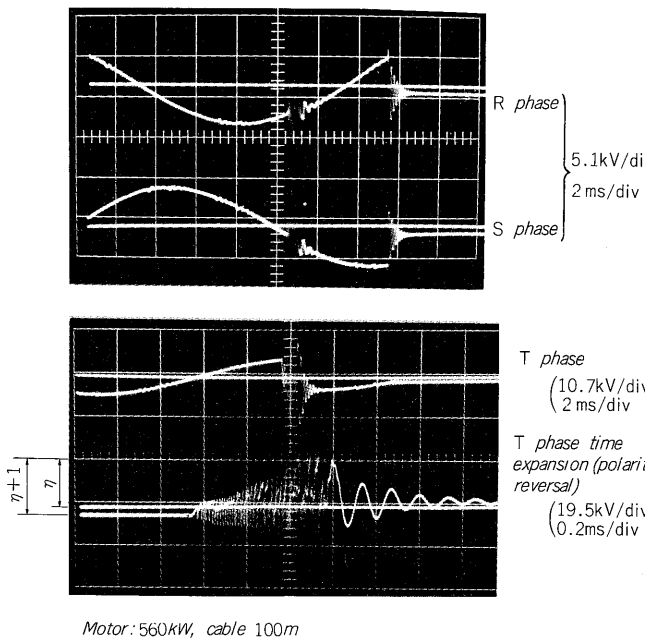


Fig. 5 Multiple reignition surge in 3-phase interruption

rent and no load current. The latter was performed with a 75kW motor and the generated surge was only the chopping surge shown by Eq. (1). Since there was a counterelectromotive force, a multiple reignition surge didn't occur. Surge voltage per unit  $\eta$  was 2 at most, and so it is confirmed that there is no problem. The results of the former are described in detail.

Fig. 5 is a surge measurement example at 3 phases. In this example, the first pole interruption is at T phase and the interruption ends after the multiple reignition occurs. Approx. 5ms later current is interrupted simultaneously at R and S phases, but no surge occurs at these phases. The test was repeated 50~100 times per condition while changing the arcing time, and the effects of motor capacity and cable length were observed. The arcing time that generates reignition is 1.5~1.8ms against the maximum arcing time 3.3ms at the first pole, but all the reignition surges are not dangerous. The cumulative probability of occurrence  $P_s$  for all the tests is shown in Fig. 6(a), for example. This is the result in the 355kW motor (starting current 320A). There is no problem in a 10m cable length, but max.  $\eta = 7 \sim 8$  times are observed in the 50~200m range. The surge occurrence probability of more than  $\eta = 3$  times (which is the surge absorber sparkover voltage and described later) in Fig. 6(a) is plotted versus cable length in Fig. 6(b).

There is not much difference in the max. surge per unit, but this probability of occurrence becomes higher as the motor capacity is smaller. Since the reignition with continuous arc occurs easily at a short cable length when the motor capacity is large, both the probability and the max. surge per unit become lower. On the other hand, when the

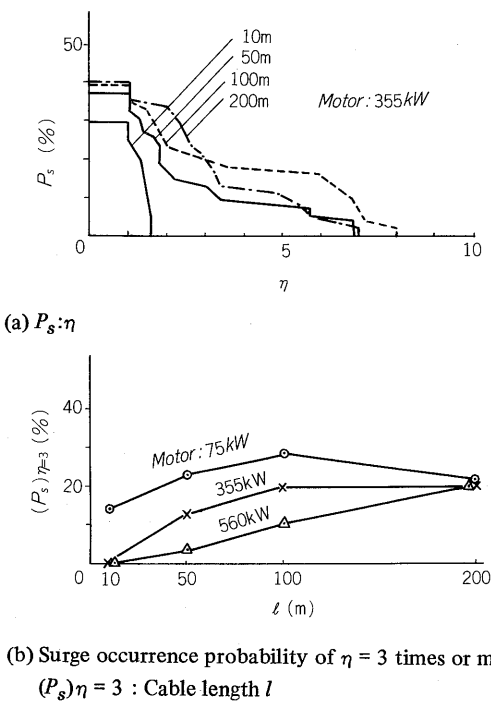


Fig. 6 Multiple reignition surge per unit ( $\eta$ ) and the cumulative probability of occurrence ( $P_s$ )

cable length is longer than 200m or so, the  $dv/dt$  of transient recovery voltage becomes smaller, and the reignition probability drops. Therefore, there is a danger region in cable length corresponding to the motor capacity.

### 2) Surge voltage distribution in motor windings

Next, the points that should be considered from the standpoint of motor insulation when a multiple reignition surge was generated are described.

Since the frequency of virtual chopping surge component of this surge is several kHz and is distributed equally by each coil, only the coil to ground insulation need to be considered for this surge magnitude per unit. However, the rise time of the reignition surge is short and the turn-to-turn insulation of coil becomes a problem because of non uniformity of voltage distribution.

Therefore, leads were drawn out from the coils of 560kW motor and the proportion of coil voltage was measured. Fig. 7 shows the proportion of surge across the first coil versus the rise time. Proportion  $\alpha$  is the one for the surge impressed between U-V, W in the figure, and  $\alpha'$  is the proportion for the surge impressed between U-G. The problem is the value of  $\alpha$  at the first pole interruption. This value is 50% even at  $t_s = 0.3\mu s$ , and is lower than the value usually considered.  $\alpha/\alpha' = 0.64$  is constant. This is because that the surge across U-G becomes 1/1.5 of the surge across U-V, W, being divided by 3 phase balanced C to ground. Then  $\alpha$  is  $\alpha'/1.5$ .  $\alpha'$  roughly coincides with the value usually considered.

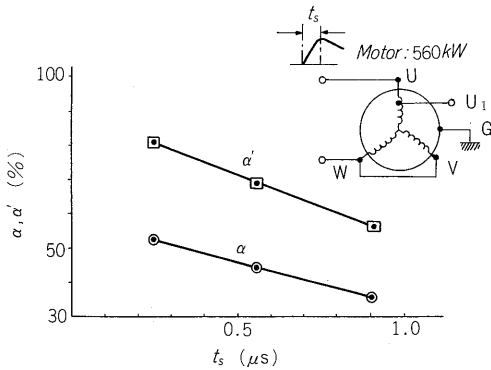


Fig. 7 Proportion of surge across the first coil ( $\alpha$ ) vs rise time ( $t_s$ )

The proportion between the turns of the first coil was also measured. In this case, the turn to turn C was substantially larger than the turn to ground C and the proportion of surge was determined by the former C. Therefore, the uniform distribution was measured in a coil up to  $t_s = 0.2\mu s$ .

The reignition surge voltage across the motor terminals and the first coil voltage when the actual cable and motor were combined are shown in Fig. 8 (analyzer test waveform).<sup>(1)</sup> Fig. 9 shows the frequency  $f_s$  versus cable length curve. (The damping factors  $\beta_1, \beta_2$  of the high frequency 1st and 2nd halfwaves at ignition are also shown in Fig. 9.)

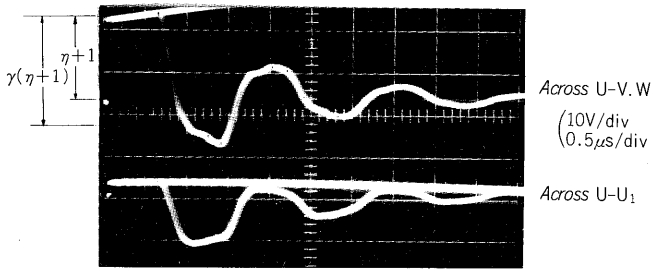


Fig. 8 Surges of motor winding and the first coil when cable connected

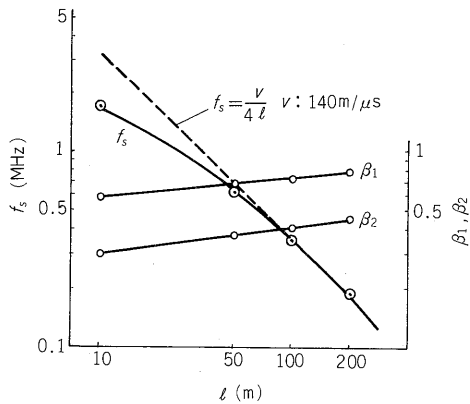


Fig. 9 Frequency ( $f_s$ ) and damping factors ( $\beta_2, \beta_1$ ) of ignition surge

The lumped constants have little effect on the surge waveform at cable lengths of 50m or longer and approaches square wave oscillation and becomes a frequency of  $f_s \simeq v/4l$  ( $v$ : traveling wave velocity,  $l$ : cable length). The surge rise time at the first coil is  $0.3\sim 0.4\mu s$  even when  $l$  is changed. The proportion at this rise time is 50% and coincides with  $\alpha$  of Fig. 7. The amplitude rate  $\gamma$  at the initial rise part of the ignition voltage ( $\eta+1$ ) is constant at approximately 1.3.

From the above, turn-to-turn surge per unit  $\eta_t$  is represented by the following Eq., where ( $\eta+1$ ) is the surge per unit across the motor windings when the surge per unit to ground is  $\eta$ .

$$\eta_t = \alpha \cdot \gamma \cdot (\eta + 1)/N \tag{3}$$

- Where,  $\alpha$ : First coil proportion  $\simeq 0.5$  ( $t_s = 0.3\mu s$ )
- $\gamma$ : Ignition surge amplitude rate  $\simeq 1.3$
- $N$ : Number of turns of first coil

For example, when suppressed to  $\eta=3$  by a surge absorber,  $\eta_t = 2.6/N$ .

3) Occurrence range of multiple reignition surge  
First, when the motor capacity is large, reignition with continuous arc occurs easily and its limit is found. When reignition occurred at  $t=t_0$  after first pole interruption, the current  $I_0$  remaining at the load  $L$  and the high frequency current  $I_s$  from the cable begin to flow in the same direc-

tion through VCB. If this current does not have a zero point, the continuous arc of a half cycle supply current is hold and a surge does not occur. The peak value of the 2nd half wave should be adopted as  $I_S$ .

$$I_0 = \sqrt{2} \cdot I \cdot \omega \cdot t_0$$

$$I_S = \beta_2 \cdot \frac{(\eta+1)Em}{1.5Z_1}$$

$I$ : Breaking current (eff)  
 $Em$ : Phase voltage crest value  
 $\beta_2$ : Damping factor of 2nd half wave (Fig. 9)  
 $Z_1$ : Cable surge impedance  
 Consequently, from  $I_0 \leq I_S$ , the surge occurs in the following,

$$I \leq 1.5 \cdot 10^{-3} \cdot \frac{\beta_2}{Z_1} \cdot \frac{(\eta+1)Em}{t_0} \dots\dots\dots (4)$$

Here,  $(\eta+1)Em/t_0$  means the dielectric recovery of the VCB.

In an experiment of 560kW motor {  $48 \times 10^6$  (V/s),  $Z_1 = 60\Omega$ , and  $\beta_2 = 0.4$  ( $l = 50m$ ) }, the condition of surge occurrence is  $I \leq 480A_{eff}$ . This coincides with the starting current of this motor and also coincides with the data of Fig. 6 (b). When the cable is short, the frequency of  $I_S$  becomes high, interruption cannot be performed at the 2nd half wave,  $\beta_2$  of Eq. (4) becomes equivalently smaller and reignition with continuous arc tends to occur.

The upper limit of the cable length for surge occurrence is found from the condition that the transient recovery voltage  $e_r$  exceeds the dielectric recovery of the VCB.

$$e_r \simeq 1.5 \cdot Em \left( 1 - \cos \frac{1}{\sqrt{L \cdot (C + lC_0)}} t \right) \dots\dots\dots (5)$$

Where,  $C_0$ : Cable capacitance per unit length  
 3-phase simultaneous interruption surge was observed in the tests of 75kW motor. Its occurrence conditions are described next. The first crest value of the high frequency current flowing into the 2nd and 3rd poles when reignition occurred at the first interrupted pole is shown by the following equation.

$$I_{S'} = \frac{1}{2} \cdot \frac{\beta_1 \cdot (\eta+1)Em}{1.5Z_1}$$

(However, this is for when only one end of cable shield is grounded, and when both ends are grounded,  $I_{S'}$  becomes larger and works adversely.)

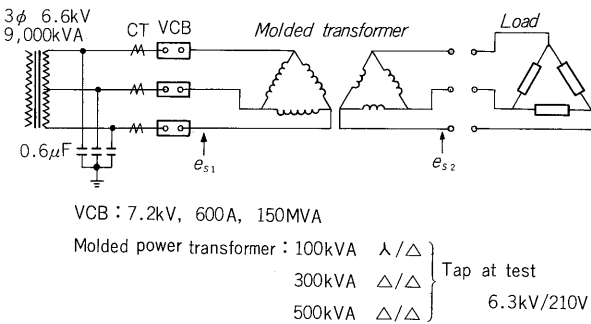
The conditions at which the current zero point appears by this  $I_{S'}$  at either the 2nd or 3rd pole is,

$$I \leq 0.272 \cdot \frac{\beta_1 \cdot (\eta+1)Em}{Z_1} \dots\dots\dots (6)$$

Where,  $\beta_1$ : Damping factor of first half wave of high frequency current (Fig. 9).

### 2. Transformer load

Fig. 10 shows the circuit in which the tests of exciting current interruption, magnetizing inrush current interrup-



Load conditions				
	Power factor	Primary $\Delta$ conversion constant		Primary current (A)
		$L$ (H/ $\Omega$ )	$R$ ( $\Omega$ )	
Series	0.49	1.93/606	216	7.0
	0.74	1.93/606	540	5.0
Parallel	0.57	2.7/848	1,296	5.8
	0.71	3.1/970	972	5.9
R	0.97	—	862	4.5

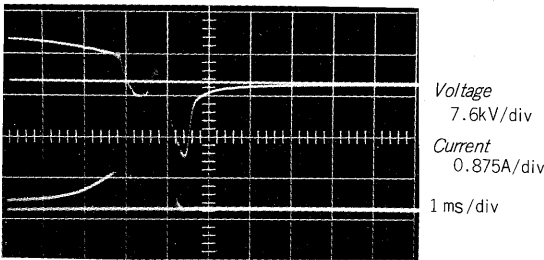
Fig. 10 Test circuit of molded power transformer

tion, and light load current interruption were performed and the surge voltage was measured. To facilitate the analysis of phenomena, a single phase test simulating first pole interruption was added as required. The measured result under each condition are described below.

#### 1) Exciting current interruption

The crest value of exciting current of 100, 300, and 500kVA molded power transformers are 1.1~2.1A and are smaller than the VCB inherent chopping current. Therefore, current chopping the occurs simultaneously at the three phases immediately after opening, and a chopping surge suppressed by reignition of several times as shown in Fig. 1 is generated. Since the current doesn't increase by repeated reignition as shown in Fig. 11 even if current chopping occurs at the rising side of the exciting current, a dangerous surge is not produced. The maximum was  $\eta = 3 \sim 4$  times for every transformer.

Fig. 12 shows the 500kVA three-phase test data. As described in 2) of item 1 of section II,  $\eta$  is determined by



Transformer: 500kVA, single phase test

Fig. 11 Surge at exciting current interruption

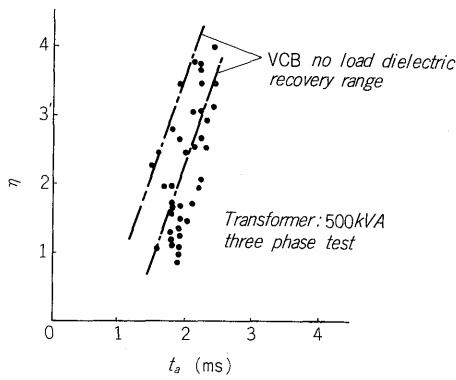


Fig. 12 Surge level per unit ( $\eta$ ) vs reignition arcing time ( $t_a$ )

recovery characteristics of dielectric strength of the VCB in the case of no load corresponding to the arcing time. The reignition arcing time is at most 2.4ms and  $\eta$  corresponding with that poses no special problem.

### 2) Magnetizing inrush current interruption

The crest value of magnetizing inrush current at three phases is (46~140), (131~406), and (152~534) A for capacities of 100, 300, and 500kVA, respectively, and it is damped to normal exciting current at about 1~30 seconds. When such a magnetizing inrush current is interrupted immediately after VCB closing, the same multiple reignition surge as a motor occurs and since the surge impedance is large, the chopping surge of 1) of item 1 of section II also poses a problem. Therefore, a protection device is necessary when interrupting a magnetizing inrush current.

### 3) Light load current interruption

Interruption test of a 15~25% light load current at a capacity of 300kVA were performed. The load is usually considered to be R-L parallel combination, but tests were also performed for a series load for the purpose of comparison. The power factor  $\cos \theta$  was also changed 0.5~0.97 and its effects investigated.

A waveform shown in Fig. 13. (a) is an example of a series load. Since the surge is large, it is accompanied by reignition, but it is the normal chopping surge and the frequency is 4kHz. On the other hand, (b) is an example of a parallel load and shows a waveform of voltage with the damping voltage DC component superimposed on an approximate 30kHz high frequency surge.

The current chopping surge is calculated by assuming the equivalent single phase circuit as shown in Fig. 14.

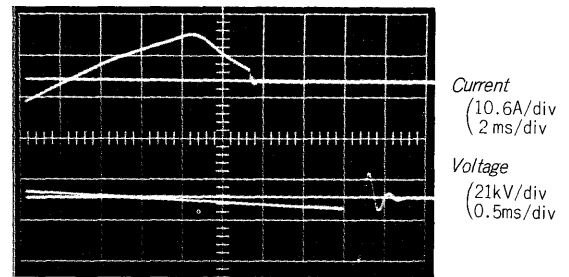
#### (1) Series load

If  $Z = \sqrt{\frac{L+L_0}{C_0}} \simeq \sqrt{\frac{L}{C_0}}$  and  $R \ll Z$  and  $E^2$  in Eq. (1) is

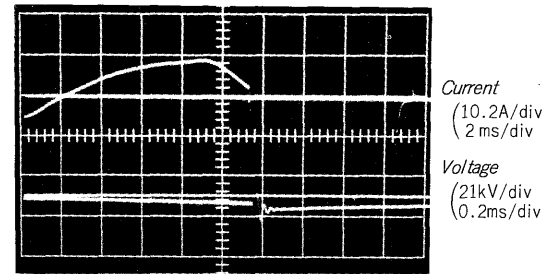
ignored,

$$e_s \simeq Z \cdot I_C \cdot \sin \frac{1}{\sqrt{L \cdot C_0}} t \quad \dots \dots \dots (7)$$

In the measurement example,  $C_0 = 1500\text{pF}$ ,  $L = 1.93\text{H}$  and the calculated frequency coincides with the measured

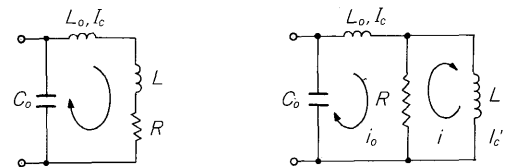


(a) Series L, R



(b) Parallel L, R

Fig. 13 Switching surge of light loaded molded power transformer interruption



(a) Series

(b) Parallel

Where,  $L_0$ : Leakage inductance

$C_0$ : Interwinding capacitance

$L$ : Primary conversion load inductance

$R$ : Primary conversion load resistance

Fig. 14 Equivalent single phase circuit of loaded transformer interruption

surge frequency. Represented by power factor  $\cos \theta$  and load current crest value  $I_m$ , the surge level per unit  $\eta$  in this case is,

$$\eta = \frac{I_C}{\sqrt{E_m \cdot \omega \cdot C_0}} \cdot \frac{(1 - \cos^2 \theta)^{1/4}}{\sqrt{I_m}} \quad \dots \dots \dots (8)$$

$\eta$  becomes larger as the power factor worsens or the load becomes smaller.

#### (2) Parallel load

If the chopping current in  $L_0$  at  $t = 0$  is  $I_C$ , the chopping current in  $L$  is  $I'_C$  and the voltage of  $C_0$  is  $E_0$ , the surge voltage  $e_s$  is approximated by the following equation.

$$e_s = Z_0 \cdot I_C \cdot e^{-\frac{R}{2L_0}t} \cdot \sin \frac{1}{\sqrt{L_0 \cdot C_0}} t + R \cdot I_C' \cdot e^{-\frac{R}{L}t} + E_0 \dots\dots\dots (9)$$

Where  $Z_0 = \sqrt{\frac{L_0}{C_0}}$

$$I_C' = I_m \left\{ \frac{I_C}{I_m} (1 - \cos^2 \theta) + \cos \theta \sqrt{1 - \cos^2 \theta} \cdot \sqrt{1 - \left( \frac{I_C}{I_m} \right)^2} \right\} \dots\dots\dots (10)$$

Where  $\frac{R^2 C_0}{L} \ll 1, R \ll 2Z_0$

Term 1 of Eq. (9) is based on the energy  $L_0 I_C^2 / 2$  discharged through the circuit  $L_0 - R - C_0$ . In the measurement example,  $L_0 = 19.6\text{mH}$  and the calculated frequency agrees with the actual high frequency component of surge. Item 2 is based on the energy  $L \cdot I_C'^2 / 2$  discharged through the circuit  $L - R$ , and represents the DC damping voltage. The surge level per unit  $\eta$  is given by the following equation.

$$\eta \simeq \frac{Z_0 I_C}{E_m} + \eta' + \frac{E_0}{E_m} \dots\dots\dots (11)$$

Where,  $\eta' = \frac{R I_C'}{E_m} = \frac{1 - \cos^2 \theta}{\cos \theta} \cdot \frac{I_C}{I_m} + \sqrt{1 - \cos^2 \theta} \cdot \sqrt{1 - \left( \frac{I_C}{I_m} \right)^2} \dots\dots (12)$

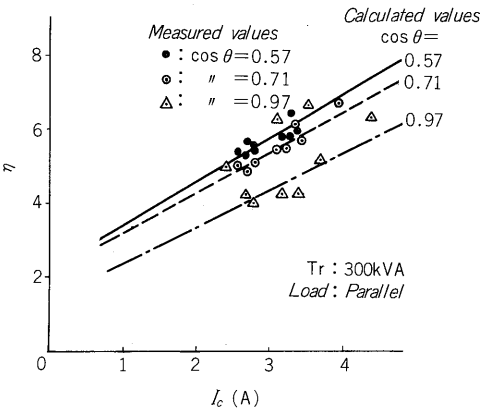


Fig. 15 Surge level per unit ( $\eta$ ) vs chopping current ( $I_C$ )

From Eqs. (11) and (12), the effect of the power factor and load current is only for term  $\eta'$  and  $\eta$  becomes larger as the power factor worsens or the load becomes smaller and  $I_C / I_m$  becomes larger. However, at a power factor of 0.5 or greater, term 1 is dominant and the power factor causes very little difference. At 1st pole interruption, terms 1 and 2 of Eq. (11) become 1.5 times respectively.

Fig. 15 is a comparison of the measured value and calculated value of  $\eta$ .

At power factors 0.57 and 0.71 the both values generally agree. The higher measured value at 0.97 is considered to be due to the effect of the magnetizing inductance.

Since the surge impedance  $Z$  of Eq. (7) is considerably larger than  $Z_0$  of Eq. (9), when series load and parallel load

Table 1 Kinds of protection method

Protector	Circuit diagram	Protection effect			Advantages and disadvantages
		Chopping surge	High frequency multiple reignition surge		
			Peak value	Rising rate	
C-R surge absorber		Double the phase voltage crest value	Double the phase voltage crest value	Noticeably reduced (1/6~1/8)	1) Ideal conditions. 2) Good protection effect. 3) Large dimensions, high price. 4) High capacitance to ground.
LA (Distribution use or substation use lightning arrester)		Five times the phase voltage crest value		Cannot be reduced.	1) Rise of sparkover voltage for large steep front surge due to V-t characteristic of gap.
ZnO (gapless surge absorber)		3.6 times the phase voltage crest value	3.6 times the phase voltage crest value	Cannot be reduced.	1) Small, light weight. 2) Fast response speed.
Reactor		75~85% of that without a reactor.	Suppressed to about 85% of the surge without a reactor.	Reducing effect.	1) Effective when the cable is short. 2) Applicable to low capacity circuits. 3) Applicable for VS use.

are compared,  $\eta$  of the series load is large, and this agrees with the measured results. Even at a parallel load, care must be exercised at a low capacity transformer because of its large  $Z_0$ .

#### IV. NEW SURGE ABSORBER AND ITS APPLICATION

##### 1. Surge protection methods

As described above, a high surge voltage that injures the insulation of the machines and apparatus is generated under certain specific conditions. Various protection device have been used to protect machines and apparatus against such a surge. *Table 1* lists some typical protectors.

###### 1) C-R surge absorber

This consists of a series capacitor and resistor connected in parallel with the load. The capacitor reduces the load side surge impedance and decreases the current chopping surge voltage. The effect of the capacitor also suppresses the rise of the surge voltage and multiple reignition surge is prevented by producing a continuous arc by adding the DC current from the capacitor to the high frequency current that flows at reignition. The series resistor attenuates the high frequency current and makes multiple reignition still more difficult.

The C-R surge absorber has the highest protection effect of all the protectors shown in *Table 1* and is widely used to protect medium voltage motor. However, it is large and expensive.

###### 2) Lightning arrester

The lightning arrester limits the surge voltage entering the electrical equipment to less than the allowable dielectric strength of the load by cutting the peak of the surge voltage. However, the residual voltage of a lightning arrester is generally based on the insulation level of the system and this is advantageous where the dielectric strength is high and known, such as a transformer, for example. However, it is not suitable for the protection of low dielectric strength machines, such as rotary machines.

###### 3) ZnO absorber

This is a so-called gap-less arrester made of a sintered body primarily made of zinc oxide (ZnO), and has the same effect as the lightning arrester. Its residual voltage is lower than that of a lightning arrester and its is small, lightweight and fast response speed.

However, if the residual voltage is made low, the varistor voltage ( $V_{1mA}$ ) decrease and the leakage current at a normal system voltage becomes large and the life of the element is noticeably shortened. Therefore, ZnO absorbers could not be given a very low residual voltage from the standpoint of element life.

A surge protector must limit the surge as low a value as possible, not be deteriorated by the normal circuit voltage, and must be small, lightweight, and inexpensive, and existing surge protectors have advantages and disadvantages.

The Fuji HE036-1 and HE072-1 surge absorbers (called SA hereinafter) were developed to solve these problems.

##### 2. Dielectric strength of protected equipment

The dielectric strength of the device to be protected

**Table 2** Insulation level of medium voltage transformer and motor

Nominal voltage		3.3kV			6.6kV		
Withstand voltage		Power frequency (for 1 minute)	Lightning Impulse ( $1 \times 40\mu s$ )		Power frequency (for 1 minute)	Lightning Impulse ( $1 \times 40\mu s$ )	
			Full wave	Chopping wave		Full wave	Chopping wave
Oil immersed transformer	No. A	16kV	45kV	50kV	22kV	60kV	65kV
	No. B	10kV	30kV	—	16kV	45kV	—
Molded power transformer*	No. A	16kV	45kV	50kV	22kV	60kV	65kV
	No. B	10kV	30kV	—	16kV	45kV	—
Dry transformer		10kV	**	—	16kV	**	—
Rotary machine		7.6kV	Not stipulated		14.2kV	Not stipulated	

Note) \*: Molded power transformer is a dry transformer according to the standards, but since the insulation level is guaranteed to be equal to that of an oil immersed transformer, it is handled as an oil immersed transformer.

\*\* : This value is for when specially requested and is not generally guaranteed.

must be considered to determine how to set the residual voltage of the SA.

###### 1) Dielectric strength according to standards

Generally, various standards demand an insulation level such as that shown in *Table 2*.

There is various opinions upon the optimum protection level for switching surges is placed is not definite, but there is a <sup>(2)</sup>study that the machine is not deteriorated by switching surge impression in the endurance life if the rising rate of voltage is comparatively low and the switching surge is lightning impulse withstand voltage  $\times 0.83 \times 0.85$  or less. And this consequence is practically applied. Therefore, it is recommended that the above mentioned method is applied for protecting machines and devices having a definite impulse withstand voltage value.

The lightning impulse withstand voltage is currently not stipulated for rotating machines but only the power frequency withstand voltage value, such as that in *Table 3*, is given. And the power frequency withstand voltage value is stipulated in the Technical Standards for Electrical Installations (Japan) as a value in which aging change has been considered as shown in *Table 3*.

There is no clear record of what strength a rotating machine has against switching surges. However, in the United States, IEEE (old AIEE) recommends a strength of 1.25 times the power frequency withstand voltage (for 1 minute), and this has been generalized.

Therefore, if the protection level is decided by consid-

**Table 3** Insulation level of medium voltage motor

Rated voltage $E$	3.3kV	6.6kV
Power frequency withstand voltage $1.5E \cdot \sqrt{2}$ (peak value) for 10 minutes	7kV	14kV



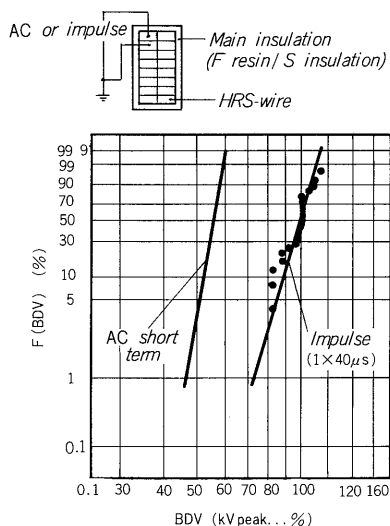


Fig. 16 Break down voltage between wiring insulated with HRS-wire

ering the IEEE recommended value and safety ratio based on the value of Table 3, protection of new and used rotating machine is obtained.

Therefore, development was performed by making the target suppressed voltage by the Type HE SA at about 3 times.

2) Dielectric strength of machines and devices of Fuji Electric

(1) Medium voltage rotating machine

1 Surge breakdown voltage

Test results of breakdown voltage of the insulation of the heat resistive synthetic resin based double-glass-fiber-covered wire (called HRS-wire hereinafter), which is used in coils of Fuji 6kV class rotating machines are shown in Fig. 16.

The  $1 \times 40 \mu s$ , breakdown voltage of positive impulse voltage is 3.5 times or more of the peak value of rated voltage, and the dielectric strength is sufficient. The AC short term breakdown voltage is also shown in Fig. 16. From the result, the impulse ratio  $IR^*$  (Impulse Ratio:  $IR$ ) is 1.8 ( $*IR = \text{impulse breakdown voltage} / \sqrt{2} \times \text{AC short term breakdown voltage}$ ). The breakdown voltage by surge voltage is considered to be changed by the waveform (mainly the duration of front form of wave:  $T_f$ ), but since  $IR$ , of course, also rises if  $T_f$  is short, adoption of the value of Fig. 16 is on the safe side even for the high rising rate of voltage that the duration of front wave is shorter than  $1 \mu s$ .

(2) Change of dielectric strength by repeated impression of surge voltage

The impulse breakdown voltage value of the cumulative probability of 50% breakdown value in Fig. 16 was made 100% and voltages of 90, 75, 65% and 60% were impressed between the turn insulation and the number of repetitions of the test voltage ( $V$ ) up to breakdown was measured.

This characteristics (so-called  $V-N$  characteristic) is

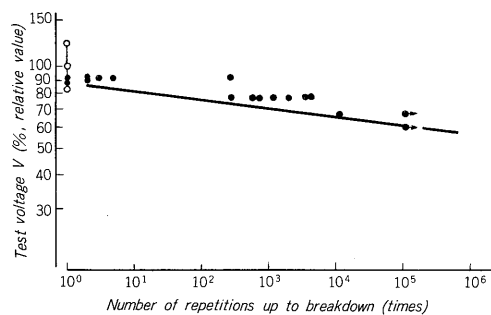


Fig. 17 Repeated impulse voltage endurance of HRS-wire

shown in Fig. 17. It can be seen that the impulse breakdown voltage does not drop even when a test voltage of 60% is impressed  $10^5$  times.

The HRS-wire above mentioned has an surge endurable characteristics. However, thermal aging, deterioration by partial discharge at the adjacent wires, etc. must be considered at machine operation. However, ample studies were made on these various characteristics and maintenance of high dielectric strength for a long time was confirmed.

If the surge voltage is suppressed by SA to 3 times or less, the proportional surge multiplier of the 1st coil becomes  $2.6/N$  as described in item 2 of para. 1 of Section III. For example, if the constitution of turn conductor is  $2 \times 10$  zigzag star connection, the surge multiplier is approximately 0.4 times even between turns having the highest voltage proportion. Because of the dielectric strength of the HRS-wire, at this voltage there is no problem for surges.

Table 4 Characteristics of molded power transformer

Feature	Reason for the feature
Non-inflammability	The resin is mixed with an inorganic filler that provides a self-extinguishing effect.
Low noise	The noise produced by the magnetic distortion of the core has been substantially reduced below that of existing Class H insulation dry transformers by noise shielding by molded coils arranged around the core.
Small size, lightweight	Since the insulation of each part of the winding depends on an electrically superior resin layer, the insulation dimensions are smaller than those of the conventional Class H insulation dry transformer and the entire transformer is small and light-weight.
High quality insulation	Since the winding is completely embedded in resin, there is virtually no drop in the insulation performance due to moisture and dust.
Rugged construction	Since the primary winding and secondary winding are both unitized by resin, they are extremely strong.
Easy maintenance and inspection	Checking by draining the insulating oil, such as with an oil immersed transformer, is unnecessary and maintenance and inspection are simple.

**Table 5** Comparisons of main insulation materials on various transformers

	Epoxy resin	Air	Mineral oil
Specific weight	1.80	$1.17 \times 10^{-3}$	0.87~0.91
Volume specific resistance ( $\Omega \cdot \text{cm}$ )	0.30	0.0221	0.107
Volume specific resistance ( $\Omega \cdot \text{cm}$ )	$0.7 \times 10^{16}$	—	$5 \times 10^{12}$
Specific inductive capacity	4.1	1.0	2.3
Breakdown voltage (kV/mm)	40	3	28 (70kV, 2.5mm)

(2) Molded power transformer

The moulded transformer developed and placed on the market by Fuji before other companies in Japan in 1974 has many features (refer to Table 4) and its popularity due to the reliability evaluation backed by a record of achievements in the field is remarkable.

If the Fuji molded power transformer is viewed from the standpoint of insulation performance,

- 1 Epoxy resin having superior insulation performance is used as the insulation material (Table 5).
- 2 The cating method which provides an ample insulation thickness is used.
- 3 The winding construction has a large series capacity and the surge voltage characteristic is improved.
- 4 Insulation design is considered long-term operation from field mapping and  $V$ - $t$  characteristics.

Because of these features, the transformer has an ample margin for the guarantee value of Table 2.

○ Molding method

Currently, there is a casting method and impregnation method of manufacturing the molded winding of so-called molded transformers in Japan.

The casting method is injection molding of the winding with resin by using a mold. It has been widely used for support insulators, bushings, potential transformers, etc. for sometime. From the standpoint of field damping and mechanical shock strength, this method can produce a resin layer of the ideal thickness depending on the mould. This method is perfect for high voltage windings. This method is used by Fuji Electric.

On the other hand, with the impregnation method the circumference of the coil is covered with external insulation, immersed in a tank of resin, and the area surrounding the coil is impregnated with a resin layer and hardened. A thin resin layer is formed by this method.

○ Winding construction

Classifying the wire of transformer windings, there is round wire (or flat square wire) and strip conductor. If both methods are compared from the standpoint of characteristics, there is a large difference at the impulse voltage characteristic.

The potential distribution inside the winding when an

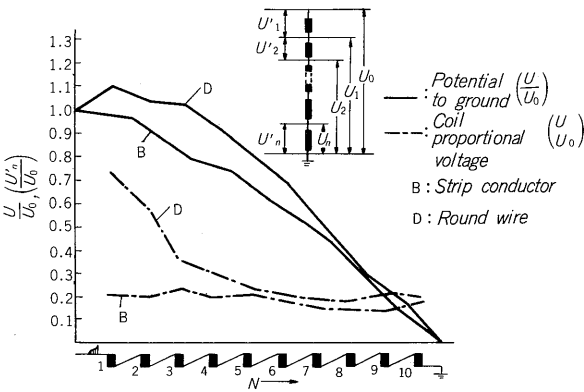


**Fig. 18** Interval voltage distributions

impulse voltage was applied is shown in Fig. 18. In the case of strip conductor, the series capacitance of the winding is large, and since the initial potential distribution of the impulse voltage is good, the potential rise caused by the internal potential vibration is much better than that of round (or flat square) wire.

Therefore, regarding the insulation against impulse voltage, strip conductor is far more advantageous than round (or flat square) wire.

○ Insulation design

As the electrical responsibility of a molded transformer there is insulation test at shipment, AC voltage operation and external surges, switching surges and other abnormal voltages during operation.

In insulation design, first the electrical stress of each part when these voltages are impressed must be found. This electrical stress is found at high precision from potential field mapping by computer, etc. Fig. 19 shows an example of potential field mapping of the main insulated parts of a Fuji molded power transformer.

On the other hand, concerning the insulation performances of the epoxy resin that forms the main insulation of the molded power transformer, in addition to the initial breakdown voltage, Fuji Electric has fully investigated the  $V$ - $t$  characteristic as the long-term insulation performance.

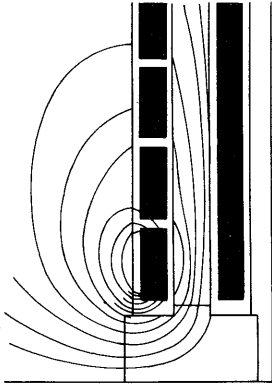


**Fig. 19** Potential field mapping

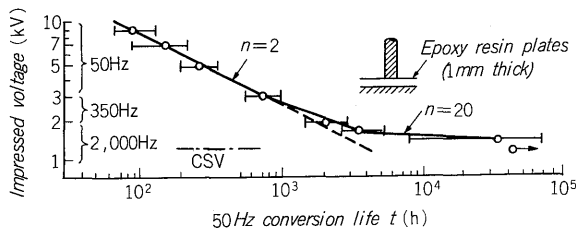


Fig. 20 *V-t* characteristics of surface discharge deterioration on epoxy resin plates

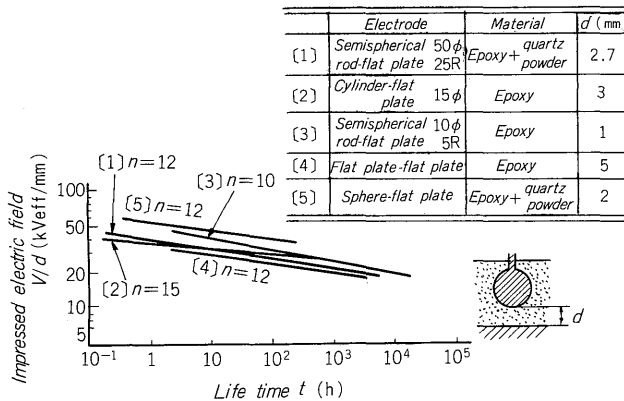


Fig. 21 *V-t* characteristics of epoxy resin molds without void and field concentration

Fig. 20 is an example of the *V-t* characteristic for epoxy resin plate and Fig. 21 is the *V-t* characteristic without void and field concentration.

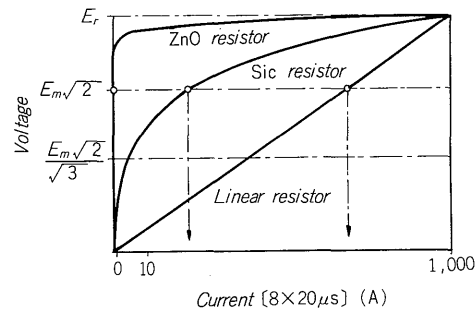
The insulation performances of the epoxy resin layer after long use can be determined by means of these *V-t* characteristics. The Fuji molded power transformer has insulation performances grasped in this manner and a high reliability insulation design considering expected life by checking the electric stress of each part obtained from the results of the field mapping described above.

### 3. Construction and functions of new Type SA

The new Type SA consists of a spark gap and a resistor having excellent nonlinearity. Both elements are arranged at the top and bottom in the vertical direction inside a plastic tube. The inside of the tube is filled with epoxy resin and both elements are sealed and completely separated from the atmosphere.

Zinc oxide (ZnO) resistors having a superb voltage-current characteristic (*V-I* characteristic) is used as the non-linear resistors.

The ZnO resistors have a curved *V-I* characteristic better than silicon carbide (SiC) resistors used as the characteristic element of conventional lightning arresters. Fig. 22 shows the *V-I* characteristic of a ZnO resistor, SiC resistor and linear resistor. In Fig. 22, the residual voltage of each is equal for an  $8 \times 20 \mu\text{s}$  waveform peak 1000A impulse current. In this case, the protective effect of each resistor is the



$E_r$ : Residual voltage

$E_m\sqrt{2}$ : Crest value of maximum permissible system voltage

(This only occurs across the absorber in the event of an earth-fault.)

$E_m\sqrt{2}/\sqrt{3}$ : Crest value of maximum power-frequency voltage across absorber during normal operation

Fig. 22 Voltage-current characteristics for different types of resistors

same. However, when compared for continuous system voltage ( $E_m$ ), the results are largely different. In short, the magnitude of the current Fig. 22 Voltage-current characteristics for different types of resistors that flows in the resistor as shown by the arrow in Fig. 22 is different and becomes lowest and almost zero for a ZnO resistor. Because it has such a superb characteristics, ZnO resistor are widely used alone as gapless arresters. However, when the residual voltage is set low, the spark over voltage (Varistor voltage:  $V_{1mA}$ ) of the ZnO resistor also becomes low and the ZnO resistor is destroyed by the leakage current at  $E_m$ . Therefore, the residual voltage of the new Type SA is adjusted low and the spark over voltage as an SA is adjusted high by using with a spark gap.

The superb *V-I* characteristic of the ZnO resistors also makes light the duty of the spark-gap. Therefore, the spark-gap of the SA is smaller than the spark-gap of conventional lightning arresters with SiC resistor and discharge delay of the SA is not a problem even for steep front surges having a rise of  $1 \mu\text{s}$  or less that are generated at high frequency reignition.

When a surge invades, the spark-gap first sparkover (discharges) and current flows to earth through the ZnO resistor. At this time, the surge is suppressed with high speed to a safe value for the insulation of the rotating machine by the *V-I* characteristic of the ZnO resistor.

After the surge has suppressed, the ZnO resistor abruptly prevents follow current by the power frequency voltage. In the case of 7.2kV rated voltage, this follow current is 5A or less. This comparatively small current is interrupted by the spark-gap at the current zero point. When this surge disappears, the ZnO resistor and spark-gap return to the initial state.

### 4. Performances and effect of the new type SA

#### 1) Ratings

The characteristics values of the new type SA are shown in Table 6 and exterior views are shown in Fig. 23. Two types, one for 3.3kV circuits and the other for 6.6kV circuits, are available as standard types.

Table 6 Ratings of new type surge absorber

Model	HE 036-1	HE 072-1
Rated voltage	3.6kV	7.2kV
100% impulse sparkover voltage (1×40μs)	8kV	15kV
Residual voltage 8 × 20μs, 1,000A	8kV	15kV
Current impulse withstand 8 × 20μs	5kA	5kA
Weight	0.6kg	0.6kg

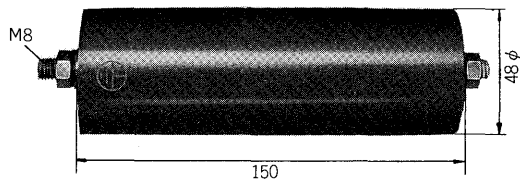


Fig. 23 Exterior view of new type surge absorber

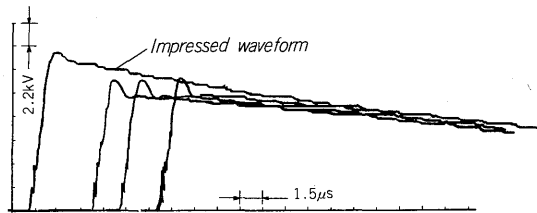


Fig. 24 Oscillogram of standard lightning-voltage impulse sparkover tests

To certify the basic performances of the new type SA, a lightning-voltage impulse sparkover test, residual voltage test, and other tests complying with JEC 203 are performed and results that should be satisfactory were obtained. Fig. 24 is an example oscillogram of the impulse sparkover voltage test and Fig. 25 is an example oscillogram of the residual voltage test.

## 2) Combined tests: Protection effect of the SA

To certify the protection effect of the SA, especially against multiple reignition surges, performances certification was performed by actually combining the SA with a medium voltage motor, and its superior performances were confirmed.

Fig. 26 shows a sparkover example. (a) is an example of suppressing the multiple reignition surge at first interrupted pole to 13.3kV ( $\eta = 2.5$  times) by this SA. When the element resistance recovers nearly the same value as surge impedance of the load after absorbing the surge energy in operation, the surge is dampened while oscillating at the chopping surge frequency.

The absorption energy  $\Delta E$  at this time is found from the following equation.

$$\Delta E = \frac{V_1 \cdot I_1 \cdot \Delta t}{(k + 2) \left(1 - \frac{V_0}{V_1}\right)} \quad \dots \dots \dots (13)$$

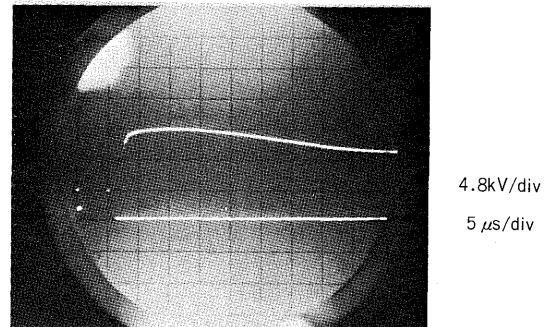
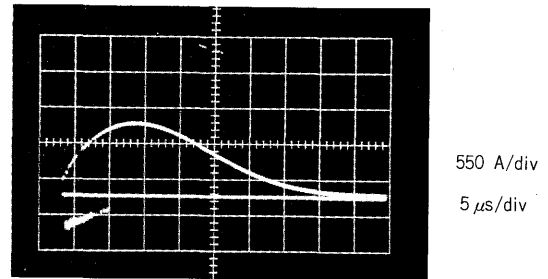
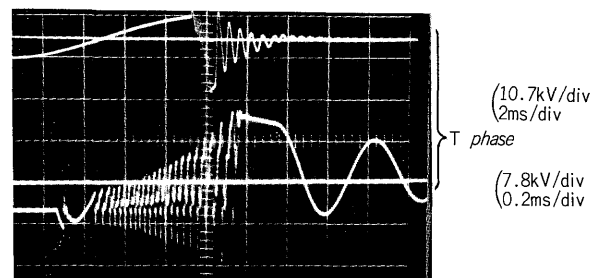
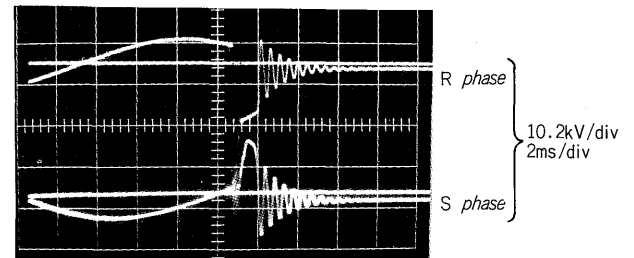


Fig. 25 Oscillogram of residual voltage tests



(a) Sparkover example at 1st pole



(b) Sparkover example at 2nd and 3rd poles at 3phase simultaneous interruption

Fig. 26 Surge suppressed by the SA

- Where,  $V_1$ : Sparkover voltage  
 $I_1$ : SA current crest value  
 $V_0$ : Voltage changing to oscillatory waveform  
 $\Delta t$ : Time from  $V_1$  to  $V_0$   
 $k$ : Constant according to SA characteristic  
 $I \propto V^k$

The measured results were  $V_1 = 12.5 \sim 15.5$ kV ( $\eta = 2.3 \sim 2.9$  times),  $\Delta E$  about 500J maximum and 100J or less in many cases, and it was confirmed that there were no problems from the standpoint of life.

Fig. 26 (b) is a sparkover example at the 2nd and 3rd poles when 3 phase simultaneous interruption occurs. This SA can suppress 3 phase simultaneous interruption to its residual voltage or less.

### V. PROTECTION DEVICES APPLICATION STANDARDS

The relationship of the surge generated by the VCB and the insulation strength of the machines and apparats must be considered in application of a VCB. As can be seen from the description up to here, a surge is not generated in all cases, but is generated when certain specific conditions are established. Therefore, when these conditions are not established by the system operating conditions, a protection device is not specially needed.

Based on our experiments, the protection application standards for the Fuji vacuum circuit breaker, considering the actual system operating conditions, are listed in Table 7.

### VI. CONCLUSION

The above has reported on VCB generation surge and its generation mechanism, generation conditions, and protection methods.

Switching of a VCB generates a surge, but it was clarified that is no problem if suitable protection is provided.

Table 7 Application guide

	Rotating machine	Class H insulation dry transformer	Oil immersed transformer, molded power transformer
3.3kV circuit	Protected by Type HE036-1 SA. Or C-R surge absorber.	Protected by Type HE036-1 SA. Or C-R surge absorber.	Protection device unnecessary. <sup>(1)</sup>
6.6kV circuit	Protected by HE072-1 SA. Or C-R surge absorber.	Protected by HE072-1 SA. Or C-R surge absorber.	Protection device unnecessary. <sup>(1)</sup>

- Notes)
- (1) When interrupting a magnetizing inrush current and when interrupting a light load current, a protection device should be used. In this case, a standard lightning arrester is sufficient.
  - (2) When there is a semiconductor device at the load side, since the surge also appears at the low voltage side according to the turns ratio of the transformer, a suitable protection device must be provided.

This can be said to have brought application of the VCB closer. The protection methods are clear and the application range of the VCB will undoubtedly widen in the future by the development of better protection devices.

The authors will be happy if this reports serves you when applying a VCB.